



# Investigations on $\text{Eu}^{3+}$ Doped Zinc Phosphate Glasses for Photonic Applications

**B. Venkata Rao<sup>1,3</sup>, G. Venkata Chalapathi<sup>1</sup>, R. Jeevan Kumar<sup>2,3</sup>**

<sup>1</sup>Loyola Degree College, Pulivendula-516 390, A.P., India; <sup>2</sup>Department of Physics, Sri Krishnadevaraya University, Anantapur- 517 003, A.P., India; <sup>3</sup>Department of Physics, JNTU University, Anantapur-515 002, A.P., India.

## ABSTRACT

Zinc phosphate (ZP) glasses doped with different concentrations of europium ( $\text{Eu}^{3+}$ ) doped were prepared, and their luminescence spectra was investigated. Thermal properties were studied by differential thermal analysis (DTA) measurements. The phase composition of the product was verified by X-ray diffraction analysis. Structural properties were studied by FTIR and Raman spectrum. Optical transition properties of  $\text{Eu}^{3+}$  in the studied zinc phosphate glasses were evaluated in the framework of Judd–Ofelt theory. The radiative transition rates ( $A_R$ ), fluorescence branching ratios ( $\beta$ ), stimulated emission cross-sections ( $\sigma_e$ ) and lifetimes ( $\tau_{exp}$ ) for certain transitions or levels were evaluated. Red emission of  $\text{Eu}^{3+}$  exhibits mainly by the  $^5\text{D}_0 \rightarrow ^7\text{F}_2$  transition located at 612 nm. Concentration quenching was observed from fluorescence spectra. It is found to be that the lifetimes of  $^5\text{D}_0$  level increases with increase in concentration and then decreases. Intense orange-red light emission was obtained for the 2.0 mol% of  $\text{Eu}^{3+}$  ions in zinc phosphate glasses. This approach shows significant promise for use in reddish-orange lighting applications which is useful in photonics field.

**Key Words:** Zinc Phosphate glass,  $\text{Eu}^{3+}$ , Judd–Ofelt theory, Concentration quenching, FTIR

## INTRODUCTION

In recent years, researcher's motivated on glasses and their optical components especially doped with lanthanide ions. The main interest is to search and develop novel optical devices for use in lasers, sensors, displays and optical amplifiers and fibers [1]. Glasses with rare earth ions are one of the functional optical materials. Glasses are in particularly suitable for rare earth ions due to higher solubility in host glass matrix [2]. Generally, rare earth elements have been widely used to modify the host properties of functional materials due to their unique physiochemical activity.

One class of host glass materials for visible and near infrared regions are phosphate glasses. Historically, phosphate glasses have been used as a host for optical applications, because of its excellent character with a wide range of rare earths solubility and high transparency. An important issue of this phosphate glass is low chemical stability and durability [3, 4].

Among rare-earth ions,  $\text{Eu}^{3+}$  is a highly active luminescence center because of simple energy level structure, its high luminescence performance as well as being a good for site selective spectroscopy. In amorphous and crystalline materials, luminescence properties of  $\text{Eu}^{3+}$  are well investigated in order to study the materials structure and local symmetry through spectroscopic probe. Optical materials based on  $\text{Eu}^{3+}$  gives strong red in phosphors and hence phosphor materials are useful for displays, lamps, illumination devices and optoelectronic devices. To get the luminescence improvement of  $\text{Eu}^{3+}$  ion, one way is co-doped method. Proper selection of co-doped material will play an important key role in energy transfer process. From energy level analysis, it is observed that the chances for energy transfer and cooperative activation between  $\text{Eu}^{3+}$  and  $\text{Sm}^{3+}$  ions are more. By co-activating with appropriate concentration of  $\text{Sm}^{3+}$  with  $\text{Eu}^{3+}$  ion it was reported emission intense red light under UV excitation [5, 6].

Recently, Rajagukguk et al. [7] studied structural and optical characteristics of  $\text{Eu}^{3+}$  ions in sodium-lead zinc-lithium-

### Corresponding Author:

**R. Jeevan Kumar**, Department of Physics, Sri Krishnadevaraya University, Anantapur- 517 003, A.P., India; Department of Physics, JNTU University, Anantapur-515 002, A.P., India; Tel: +91 9491120089; Email: rjkskuphy@yahoo.com

**ISSN:** 2231-2196 (Print)

**ISSN:** 0975-5241 (Online)

**DOI:** 10.7324/IJCRR.2017.9134

**Received:** 23.05.2017

**Revised:** 08.06.2017

**Accepted:** 22.06.2017

borate glass system and concluded that decay time increases with increasing  $\text{Eu}^{3+}$  ion concentration. Ouchouicha et al. [8] prepared  $\text{Eu}^{3+}/\text{Eu}^{2+}$  co-doped calcium aluminosilicate glass-ceramics and observed that during heating of the original glass, part of  $\text{Eu}^{3+}$  ions were reduced to  $\text{Eu}^{2+}$  ions. Steudel et al. [9] investigated quantum efficiency and energy transfer (ET) processes in rare-earth doped borate glass for solid-state lighting and concluded that for constant  $\text{Sm}^{3+}$  concentration and increasing  $\text{Eu}^{3+}$  doping, the efficiency increases slightly.

The present paper focused on the systematic characterization and analysis of concentration effect of  $\text{Eu}^{3+}$  on luminescence and. Thermal, structural and optical aspects of zinc phosphate glasses were done by DTA, XRD, FTIR, Raman, optical absorption, emission and lifetime measurements. To study concentration effect, proper analysis of excitation, emission and energy level analysis are needed and these were recorded for  $\text{Eu}^{3+}$  doped ZP glasses.

## METHODOLOGY

Different zinc phosphate (ZP) glasses were prepared by using raw materials (99.9%), ammonium phosphate ( $\text{NH}_4\text{H}_2\text{PO}_4$ ), lithium fluoride (LiF), strontium oxide (SrO), zinc oxide (ZnO) and europium oxide ( $\text{Eu}_2\text{O}_3$ ). The glass compositions details as follows (mol%):

1 Eu01	59.9 $\text{NH}_4\text{H}_2\text{PO}_4$ -10LiF-10SrO-20ZnO-0.1 $\text{Eu}_2\text{O}_3$
2 Eu05	59.5 $\text{NH}_4\text{H}_2\text{PO}_4$ -10LiF-10SrO-20ZnO-0.5 $\text{Eu}_2\text{O}_3$
3 Eu10	59.0 $\text{NH}_4\text{H}_2\text{PO}_4$ -10LiF-10SrO-20ZnO-1.0 $\text{Eu}_2\text{O}_3$
4 Eu15	58.5 $\text{NH}_4\text{H}_2\text{PO}_4$ -10LiF-10SrO-20ZnO-1.5 $\text{Eu}_2\text{O}_3$
5 Eu20	58.0 $\text{NH}_4\text{H}_2\text{PO}_4$ -10LiF-10SrO-20ZnO-2.0 $\text{Eu}_2\text{O}_3$
6 Eu30	57.0 $\text{NH}_4\text{H}_2\text{PO}_4$ -10LiF-10SrO-20ZnO-3.0 $\text{Eu}_2\text{O}_3$

Precise amounts of the starting materials in mol% were weighed out and grinded in an agate mortar. The mixtures were placed in porcelain crucibles and were then heated in an electric furnace. After heating, the obtained liquid was poured on brass plate and then pressed by another brass plate. The obtained glasses are used for measurements.

DTA measurement was performed using a NetZsch STA 409 model with  $\text{N}_2$  atmosphere. Amorphous nature of prepared glasses was verified by SEIFERT X-RAY diffractometer. FTIR spectrum was recorded using a series of Perkin Elmer spectrum One FT-IR spectrophotometer. Raman spectrum was recorded JOBIN YVUON spectrometer. The optical absorption spectral recording was done on ELICO SL 218 double beam spectrophotometer. The excitation, photoluminescence spectra and decay curves of  $\text{Eu}^{3+}$  doped glass samples were recorded using FLS-980 fluorescence spectrometer with xenon lamp as excitation source.

## RESULTS

### Thermal analysis- Differential thermal analysis (DTA)

In order to understand and interpret the thermal, crystallization and melting behaviour of glass system, differential thermal analysis (DTA) is important one. Through DTA analysis, phase changes are also observed during thermal heat treatment. The separated various phases like glass transition temperature ( $T_g$ ) and crystallization temperature ( $T_c$ ) which are depend on the different constituting oxides such as glass former and modifiers in the glass systems. DTA profile is recorded for host ZP glass matrix and is presented in Fig.1.

### XRD analysis

XRD profile of 2.0 mol% of europium doped zinc phosphate glass is pictured in Fig.2.

### FTIR spectrum

Fig.3 shows FTIR spectrum of 2.0 mol% doped zinc phosphate glass matrix. The bands are observed at  $740\text{ cm}^{-1}$ ,  $910\text{ cm}^{-1}$ ,  $1075\text{ cm}^{-1}$  and  $1230\text{ cm}^{-1}$ .

### Raman spectrum

Fig.4 shows Raman spectrum of 2.0 mol% doped zinc phosphate glass matrix. The bands are observed between  $300\text{--}480\text{ cm}^{-1}$  region and at  $773\text{ cm}^{-1}$ .

### Optical absorption of $\text{Eu}^{3+}$ doped ZP glasses

The optical changes of the  $\text{Eu}^{3+}$  doped ZP glasses were observed through the absorption spectra and these measurements for all glasses were recorded and were shown in Fig. 5 for 2.0 mol% of  $\text{Eu}^{3+}$  doped glass matrix. The absorption spectra display seven transitions from the ground levels  $^7F_0$  and  $^7F_1$ . The absorption spectral bands originate from  $^7F_0$  and  $^7F_1$  levels since these levels ( $^7F_0$  and  $^7F_1$ ) are being closely located to each other.

### Excitation and emission spectra of $\text{Eu}^{3+}$ doped ZP glasses

The observed excitation and emission spectra of  $\text{Eu}^{3+}$ -doped ZP glasses were shown in Figs. 6 and 7 respectively. The observed excitation spectral transitions were found to be matched with the absorption transitions. In the excitation spectra, major emission intensity was observed at 393 nm due to  $^7F_0 \rightarrow ^5L_7$  transition for all  $\text{Eu}^{3+}$ -doped ZP glasses and using this as excitation source, emission spectra were recorded. Fig. 7 shows  $\text{Eu}^{3+}$  doped emission spectra for Eu01, Eu05, Eu10, Eu15, Eu20 and Eu30 glasses under ultraviolet excitation source (at 393 nm).

### Decay analysis of Eu<sup>3+</sup> doped ZP glasses

The emission decay time of the <sup>5</sup>D<sub>0</sub> level (at  $\lambda_{\text{exc}} = 393$  nm and at  $\lambda_{\text{emi}} = 612$  nm) of the different ZP glasses are shown in Fig. 8. The decay curves were fitted to the first order exponential function for all Eu<sup>3+</sup> doped ZP glasses.

## DISCUSSION

From Fig.1, an endothermic peak located nearly at 136 °C is observed which is due glass transition temperature ( $T_g$ ). Two exothermic peaks follow after the glass transition temperature indicating the stage of crystallization ( $T_c$ ) process.  $T_{c1}$  and  $T_{c2}$  are two crystallization events are formed during melting process. These two events are occurred nearly at 196 and 267 °C temperatures, respectively. From Fig. 1, where the higher  $T_{c2}$  and lower  $T_g$  are used to measure the thermal stability of the amorphous zinc phosphate glass system. The thermal stability or glass forming ability can be measured by difference of glass transition and crystallization temperatures ( $\Delta T = T_{c2} - T_g$ ) [10]. In the present work, it is observed that the thermal stability is found to be 131 °C which is high for the zinc phosphate glass system.

From this XRD figure 2, it is apparent that no characteristic diffraction peaks, indicating that the prepared glasses are of amorphous in nature. Fig.3 consists of the band at 740 cm<sup>-1</sup> is ascribed to the symmetric stretching vibration of P–O–P rings. The absorption band at 910 cm<sup>-1</sup> is related to asymmetric stretching vibration of P–O–P groups linked with linear metaphosphate chains. The band at 1075 cm<sup>-1</sup> is assigned to asymmetric stretching of PO<sub>2</sub><sup>-</sup> group units. The band at 1230 cm<sup>-1</sup> is attributed to the stretching of the doubly bonded oxygen vibration,  $\nu_{\text{as}}(\text{P}=\text{O})$  modes [11].

Fig.4 shows Raman spectrum consists of the broad band at 773 cm<sup>-1</sup> is due to symmetric stretching of (P–O–P) bridging oxygen bonds in (P<sub>2</sub>O<sub>7</sub>)<sup>4-</sup> units. [12, 13, 14]. This peak is a convolution of two peaks i.e. one may due to vibrations of the two joined Q<sup>2</sup> units and the second one to those of Q<sup>1</sup> units. Presence of last two bands indicates that due to addition of different modifiers into glass matrix, long range order of network become cut down and formed chain like units. This type of structural units increases glass strength.

The absorption spectra (Fig.5) display seven transitions from the ground levels <sup>7</sup>F<sub>0</sub> and <sup>7</sup>F<sub>1</sub>. The absorption spectral bands originate from <sup>7</sup>F<sub>0</sub> and <sup>7</sup>F<sub>1</sub> levels since these levels (<sup>7</sup>F<sub>0</sub> and <sup>7</sup>F<sub>1</sub>) are being closely located to each other. However, transitions from the <sup>7</sup>F<sub>2</sub> level were too weak to be investigated because of the minimum fractional thermal populations at room temperature [14]. The optical bands observed due to the <sup>7</sup>F<sub>0</sub> → <sup>5</sup>D<sub>4</sub>, <sup>7</sup>F<sub>0</sub> → <sup>5</sup>G<sub>4</sub>, <sup>7</sup>F<sub>1</sub> → <sup>5</sup>G<sub>3</sub>, <sup>7</sup>F<sub>0</sub> → <sup>5</sup>L<sub>6</sub>, <sup>7</sup>F<sub>1</sub> → <sup>5</sup>D<sub>3</sub>, <sup>7</sup>F<sub>0</sub> → <sup>5</sup>D<sub>2</sub> and <sup>7</sup>F<sub>1</sub> → <sup>5</sup>D<sub>1</sub> transitions, centered at 362, 376, 382, 393, 415, 465 and 535 nm respectively. At room temperature, energy difference between <sup>7</sup>F<sub>1</sub> and <sup>7</sup>F<sub>0</sub> level was only ~350 cm<sup>-1</sup> and thermally populated about 35% and 65% respec-

tively. Hence, absorption transitions were appeared from both levels [16]. So that, Judd-Ofelt analysis from the absorption spectra is very difficult. Out of these seven bands, the absorption band, <sup>7</sup>F<sub>0</sub> → <sup>5</sup>L<sub>6</sub> has more intensity than rest of the absorption bands. This transition was forbidden by the  $\Delta S$  and  $\Delta L$  selection rules, but it is allowed by the  $\Delta J$  selection rule. Furthermore, the intensity of <sup>7</sup>F<sub>0</sub> → <sup>5</sup>D<sub>2</sub> (electric dipole) transition has higher than that of <sup>7</sup>F<sub>0</sub> → <sup>5</sup>D<sub>1</sub> transition (magnetic dipole). Hence, the <sup>7</sup>F<sub>0</sub> → <sup>5</sup>D<sub>2</sub> transition is referred as hypersensitive transition [17,18].

The excitation spectra (at  $\lambda_{\text{emi}} = 611$  nm) were composed of <sup>7</sup>F<sub>1</sub> → <sup>5</sup>I<sub>5</sub>, <sup>7</sup>F<sub>0</sub> → <sup>5</sup>H<sub>6</sub>, <sup>7</sup>F<sub>0</sub> → <sup>5</sup>H<sub>3,7</sub>, <sup>7</sup>F<sub>0</sub> → <sup>5</sup>D<sub>4</sub>, <sup>7</sup>F<sub>0</sub> → <sup>5</sup>L<sub>10</sub>, <sup>7</sup>F<sub>0</sub> → <sup>5</sup>G<sub>2,3,4,5</sub>, <sup>7</sup>F<sub>0</sub> → <sup>5</sup>L<sub>7</sub>, <sup>7</sup>F<sub>0</sub> → <sup>5</sup>L<sub>6</sub>, <sup>7</sup>F<sub>0</sub> → <sup>5</sup>D<sub>3</sub>, <sup>7</sup>F<sub>0</sub> → <sup>5</sup>D<sub>2</sub>, <sup>7</sup>F<sub>0</sub> → <sup>5</sup>D<sub>1</sub> and <sup>7</sup>F<sub>1</sub> → <sup>5</sup>D<sub>1</sub> transitions with the wavelengths located at 302, 319, 326, 360, 364, 376, 381, 393, 413, 463, 522 and 531 nm respectively (Fig.6). The <sup>7</sup>F<sub>0</sub> → <sup>5</sup>L<sub>6</sub> (393 nm) and <sup>7</sup>F<sub>0</sub> → <sup>5</sup>D<sub>2</sub> (464 nm) transitions indicate relatively higher intensities than the other transitions [19]. It is observed that the peak at 440 nm is associated to the pure electronic transition (PET) and the peak at 464 nm is associated to the phonon side band (PSB) <sup>7</sup>F<sub>0</sub> → <sup>5</sup>D<sub>2</sub> occur at higher energy side. Due to excitation by the incident energy corresponding to the PET with an excess energy of vibrational modes of Eu-O bonds, PSBs were occurring. The phonon energy ( $\hbar\omega$ ) can be defined as energy difference between PSB (at 22727 cm<sup>-1</sup>) and PET (at 21555 cm<sup>-1</sup>), it was 1172 cm<sup>-1</sup> in Eu<sup>3+</sup> doped ZP glasses. Thus, PSBs result from inter mixing of vibrational modes to the IR bands in the range 1080-1270 cm<sup>-1</sup> related to P-O-P and P=O bands. The electron-phonon coupling strength parameter ( $g$ ) was calculated from the integrated intensity ratios of PSB to PET using the formula given in Ref. [20]. The  $g$  parameter gives intensity of interaction between Eu<sup>3+</sup> cation and O<sup>2-</sup> ligand anion. This  $g$  parameter was found to be 0.1, 0.4, 0.5, 0.7 and 0.5 for Eu01, Eu05, Eu10, Eu15, Eu20 and Eu30 glass matrices respectively.

In the excitation spectra, major emission intensity was observed at 393 nm due to <sup>7</sup>F<sub>0</sub> → <sup>5</sup>L<sub>7</sub> transition for all Eu<sup>3+</sup>-doped ZP glasses and using this as excitation source, emission spectra (Fig.7) were recorded. By using 393 nm excitation, transitions from ground level to <sup>5</sup>L<sub>7</sub> level take place. The population of the <sup>5</sup>L<sub>7</sub> level relaxes non-radiatively (NR) to the <sup>5</sup>D<sub>3</sub> level, and then sequentially to the lower <sup>5</sup>D<sub>0</sub> level via <sup>5</sup>D<sub>2</sub> and <sup>5</sup>D<sub>1</sub> levels. Emissions from the <sup>5</sup>D<sub>0</sub> level to lower levels takes place radiatively due to higher energy gap between the excited <sup>5</sup>D<sub>0</sub> and <sup>5</sup>F<sub>6</sub> level and negligible multiphonon relaxation (MPR) effect. Emission occurs only from <sup>5</sup>D<sub>0</sub> level and emission from <sup>5</sup>D<sub>1</sub>, <sup>5</sup>D<sub>2</sub> and <sup>5</sup>D<sub>3</sub> levels were not observed (From Fig.7) due to higher phonon energy of ZP host glass matrix. In the present work, five emission bands (in the visible region) were noticed i.e. from the excited state <sup>5</sup>D<sub>0</sub> to lower levels i.e. <sup>5</sup>D<sub>0</sub> → <sup>7</sup>F<sub>0</sub> (578 nm, yellow), <sup>5</sup>D<sub>0</sub> → <sup>7</sup>F<sub>1</sub> (590 nm, orange), <sup>5</sup>D<sub>0</sub> → <sup>7</sup>F<sub>2</sub> (611, red), <sup>5</sup>D<sub>0</sub> → <sup>7</sup>F<sub>3</sub> (653 nm, deep red), <sup>5</sup>D<sub>0</sub> → <sup>7</sup>F<sub>4</sub> (701 nm, deep red).

The emission line associated with  $^5D_0 \rightarrow ^7F_2$  transition has the highest emission intensity and the emission line associated with  $^5D_0 \rightarrow ^7F_0$  transition has the lowest in emission intensity. Out of five bands, the  $^5D_0 \rightarrow ^7F_2$  band was a forced electric dipole (ED) allowed transition and it possesses hypersensitive character due to the admixture of odd-parity character into the  $4f^6$  wave functions. Meanwhile, the  $^5D_0 \rightarrow ^7F_1$  was magnetic dipole (MD) spin-forbidden transition but it is allowed when Eu<sup>3+</sup> ion is in higher symmetric position due to spin-orbit interaction. The rest of emission lines  $^5D_0 \rightarrow ^7F_J$  ( $J = 0$  and  $3$ ) were strictly forbidden. The intensity ratio ( $R$ : ED/MD) was widely used to manifest the bonding medium and asymmetry around Eu<sup>3+</sup> ions. This ratio gives information concern covalent/ionic bonding between the Eu<sup>3+</sup> ions and the surrounding oxygen ligands. With increase in europium concentration,  $R$  value also increases due to increase in asymmetry and higher degree of covalency between Eu–O. Smaller values of  $R$  is attributed to higher local symmetry for Eu<sup>3+</sup> ions.

Increase of Eu<sup>3+</sup> content from 0.1 mol% to 2.0 mol% increases the emission intensities, and then decreases drastically when Eu<sup>3+</sup> content is 3.0 mol%. As the concentration increased, the Eu<sup>3+</sup> ions are crowded closer and closer together. This is owing to strong interactions among the europium ions as well as cross relaxation (CR) process at higher concentrations. These CR was from  $^5D_2$  to  $^5D_1$  levels and from  $^5D_3$  to  $^5D_2$  levels and channels like :  $^5D_2 + ^7F_1 \rightarrow ^5D_1 + ^7F_4$  and  $^5D_3 + ^7F_0 \rightarrow ^5D_2 + ^7F_4$ . Among all ZP glasses, 2.0 mol% of Eu<sup>3+</sup> doped ZP glass shows the strongest red emission intensity.

The limited level of absorption transitions and energy level structure of Eu<sup>3+</sup> ion, Judd-Ofelt parameters were unable to determine from absorption spectra. Hence, the J-O intensity parameters ( $\Omega_2$  and  $\Omega_4$ ) [21, 22] were calculated for Eu20 ZP glass system from the emission spectra. The  $^5D_0 \rightarrow ^7F_2$  transition has not been observed in emission spectra and hence  $\Omega_6$  parameter was not evaluated. It is observed that the  $\Omega_2$  parameter is high ( $7.11 \times 10^{-20} \text{ cm}^2$ ) in 2.0 mol% Eu<sup>3+</sup>-doped ZP glass matrix. This indicates that high asymmetry and covalency connected around the europium ions in the Eu20 glass matrix. The J-O parameters followed with trend like  $\Omega_2 > \Omega_4$  in Eu20 ZP glass. This affirmation is also in consistency with the obtained R/O intensity ratios observed in Eu20 glass matrix. J-O intensity parameters were used to assess the radiative properties and are presented in Table 1 for Eu20 ZP glass matrix.

It is observed that among all emission transitions,  $^5D_0 \rightarrow ^7F_2$  transition shows higher values of radiative transition probabilities ( $A_R$ ) in all the concentrations, and this value is high in 2.0 mol%. The experimental branching ratios ( $\beta_{\text{exp}}$ ) and stimulated emission cross-sections ( $\sigma_e$ ) for all the emission transitions of Eu<sup>3+</sup>-doped ZP glass matrices are also calculated. The  $\beta_{\text{exp}}$  are obtained from the rela-

tive areas under specific transitions. From Table 1, among all emission transitions,  $^5D_0 \rightarrow ^7F_2$  transition has higher  $\beta_{\text{exp}}$  (68%) for 2.0 mol% of Eu<sup>3+</sup>-doped Eu20 glass matrix. It indicates that the dominant red emission located at 612 nm of Eu<sup>3+</sup> might be useful for optical materials. The luminescence performance of the material can be decided from  $\sigma_p$  values. From table 1, the  $\sigma_p$  values are higher for  $^5D_0 \rightarrow ^7F_2$  transition compared to other emission transitions.

The obtained lifetimes (Fig.8) were 2.3, 2.3, 2.4, 2.5, 2.6, and 2.7 ms for Eu01, Eu05, Eu10, Eu15, Eu20 and Eu30 glasses respectively. Decay time is observed to be increased with increasing Eu<sup>3+</sup> ion concentrations from 0.1 mol% to 2.0 mol% and then decreases. The glass sample with 0.1 mol% shows the shortest luminescence lifetimes and sample with 2.0 mol% shows the longest luminescence lifetimes.

## CONCLUSION

The authors prepared and characterized Eu<sup>3+</sup> doped zinc phosphate glasses for luminescence applications. The thermal stability measured by using DTA technique. In the present work, it is observed that the thermal stability is found to be 131 °C which is high for the zinc phosphate host glass system. The phase composition of the product was verified by X-ray diffraction analysis and found to be amorphous in nature. The structural properties are studied through FTIR and Raman measurements. Optical properties of Eu<sup>3+</sup> in the studied zinc phosphate glasses were evaluated in the framework of Judd-Ofelt theory. Among different ZP glasses, Eu20 has high covalency bond. Red emission of Eu<sup>3+</sup> is generated mainly by the  $^5D_0 \rightarrow ^7F_2$  transition located at 612 nm. Concentration quenching and energy transfer were observed from fluorescence spectra and decay curves, respectively. The 0.1 mol% and 3.0 mol% Eu<sup>3+</sup> doped ZP samples have the longest and shortest decay times. With the increase in dopant concentration, decay time values gradually decreased. It was found that the main reason for concentration quenching was non-radiative energy transfer through cross-relaxation mechanism due to dipole-dipole interaction. This approach shows significant promise for use in bright orange-red lighting applications. The optimized properties of the Eu<sup>3+</sup> doped zinc phosphate glasses are found to be promising luminescent materials.

## ACKNOWLEDGEMENTS

Authors acknowledge the immense help received from the scholars whose articles are cited and included in references of this manuscript. The authors are also grateful to authors / editors / publishers of all those articles, journals and books from where the literature for this article has been reviewed and discussed.



**Source of funding:** None

**Conflicts of interest:** None

## REFERENCES

1. A.N. Meza-Rocha, G. Muñoz A. Speghini, M. Bettinelli, U. Caldiño, *Opt. Mater.* 2015, 47 (2015).
2. D. Chateau, F. Chaput, C. Lopes, M. Lindgren, C. Brannlund, J. Öhgren, N. Djourelou, P. Nedelec, C. Desroches, B. Eliasson, T. Kindahl, F. Lerouge, C. Andraud, S. Parola, *Appl. Mater. Interfaces*, 2012, 4, 2369.
3. S. Babu, A. Balakrishna, D. Rajesh, Y.C. Ratnakaram, *Spectrochimica Acta Part A*, 2014, 122, 639.
4. P. Xiao, J.J. Zhang, L.F. Shen, Z.Q. Wang, E.Y.B. Pun, H. L. in, *J. Lumin.* 2016, 178, 147.
5. Xiaofeng Wu, Shigang Hu, Congbing Tan, Yunxin Liu, *Opt. Commun.* 2014, 328, 23.
6. Ye Jin, Jiahua Zhang, Weiping Qin, *J. Alloys Compd.* 2013, 579, 263.
7. J. Rajagukguk, J. Kaewkhao, M. Djamel, R. Hidayat, Suprijadi, Y. Ruangtaweep, *J. Mol. Struct.* 2016, 1121, 180.
8. H. Bouchouicha, G. Panczer, D. de Ligny, Y. Guyot, M.L. Baesso, L.H.C. Andrade, S.M. Lima, R. Ternane, *J. Lumin.* 2016, 169, 528.
9. Franziska Steudel, Sebastian Loos, Bernd Ahrens, Stefan Schweizer *J. Lumin.* 2016, 170, 770.
10. F.Wu, S. Li, Z. Chang, H. Liu, S. Huang, Y. Yue, *J. Mole. Struct.* 1118 (2016) 42-47.
11. C. Ivascu, A. Timar Gabor, O. Cozar, L. Daraban, I. Ardelean, *J. Mol. Struct.* 2011, 993, 249.
12. M. Lu, F. Wang, Q. Liao, K. Chen, J. Qin, S. Pan *J. Mol. Struct.* 2015, 1081, 187.
13. Y.C. Ratnakaram, S. Babu, L. Krishna Bharat, C. Nayak *J. Lumin.* 2016, 175, 57.
14. K. Brahmachary, D. Rajesh, Y.C. Ratnakaram, *J. Lumin.* 2015, 161, 202.
15. M. Szumera, I. Wacławska, J. Sułowska, *J. Mol. Struct.* 2016, 1114, 78.
16. N. Mascaraque, G. Tricot, B. Revel, A. Durána, F. Muñoz, *Solid State Ionics* 2014, 254, 40.
17. P.Y. Shih, J.Y. Ding, S.Y. Lee, *Mater. Chem. Phys.* 2003, 80, 391.
18. W.A. Pisarskia, J. Pisarska, G. Dominiak-Dzik, M. Maćzkac, W. Ryba-Romanowski, *J. Phys. Chem. Solids* 2016, 67, 2452.
19. U. Caldiño, A. Speghini, S. Berneschi, M. Bettinelli, M. Brenici, S. Pelli, G.C. Righini, *Opt. Mater.* 2012, 34, 1067.
20. D. Ramachari, L. Rama Moorthy, C.K. Jayasankar, *J. Lumin.* 2013, 143, 674.
21. B.R. Judd, *Phys. Rev.* 1962, 127, 750.
22. G.S. Ofelt, *J. Chem. Phys.* 1962, 37, 511.

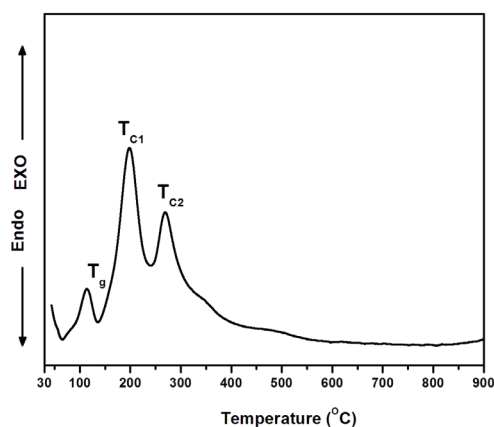


**Figure 1:** DTA profile for zinc phosphate host glass matrix.

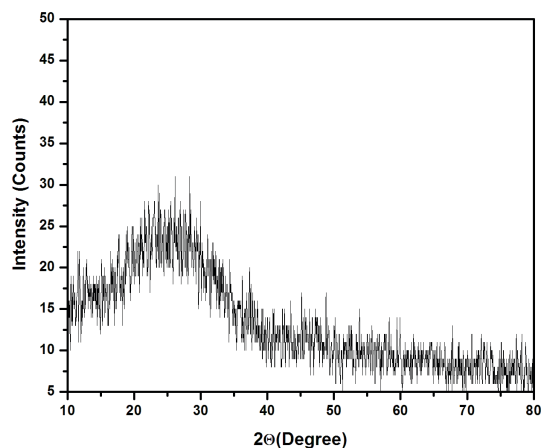


**Figure 2:** XRD profile for 2.0 mol% of europium doped zinc phosphate glass matrix.

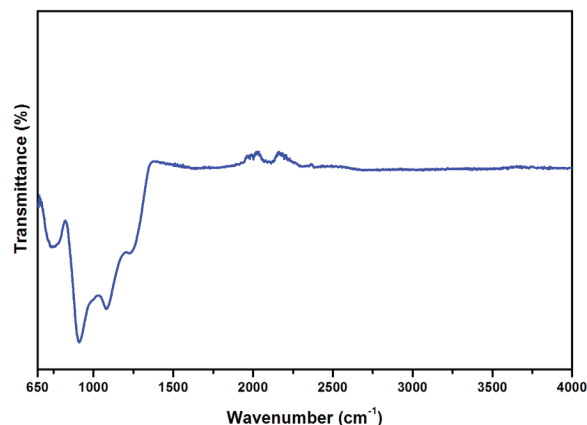


**Figure 3:** FTIR spectrum of 2.0 mol% of europium doped zinc phosphate glass matrix.

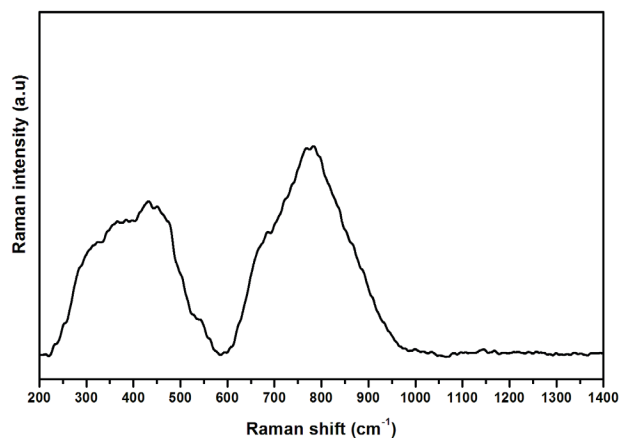


**Figure 4:** Raman spectrum of 2.0 mol% of europium doped zinc phosphate glass matrix.

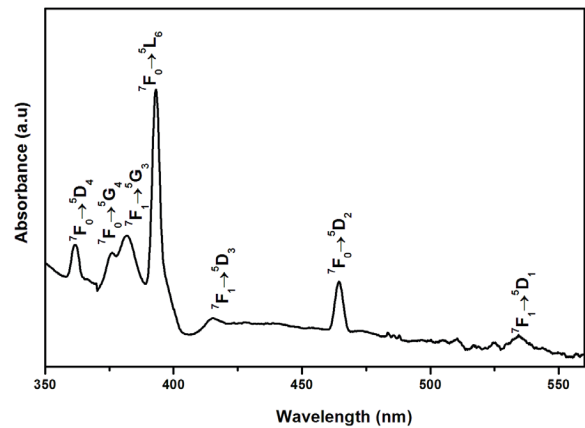


Figure 5: Absorption spectrum for 2.0 mol% of europium doped zinc phosphate glass matrix

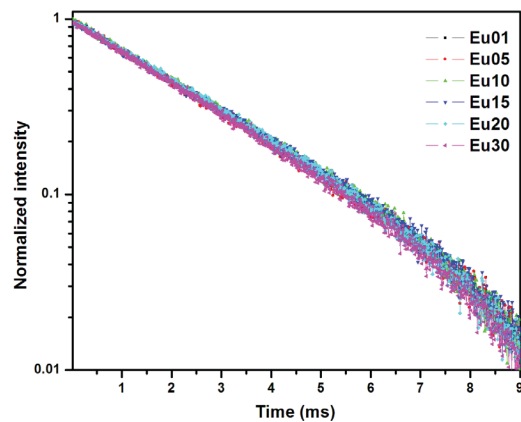


Figure 8: Decay profiles for europium doped zinc phosphate glass matrix for different concentrations

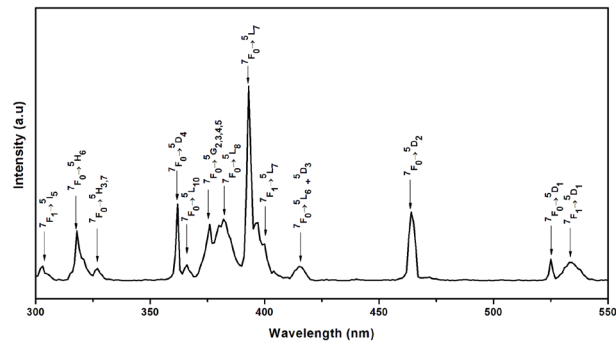


Figure 6: Excitation spectrum for 2.0 mol% of europium doped zinc phosphate glass matrix

Table 1: Radiative transition rates ( $A_R$ ,  $s^{-1}$ ), branching ratios ( $\beta_{exp}$ ) and peak-stimulated emission cross-sections ( $\sigma_p$ ,  $\times 10^{-22} \text{ cm}^2$ ) of certain emission transitions of 2.0 mol% Eu<sup>3+</sup> doped ZP glass matrix.

Glass matrix	Transition	$A_R$	$\beta_{exp}$	$\sigma_p$
Eu20	$5D_0 \rightarrow 7F_0, 7F_1$	0	1	0
	$7F_2$	45	12	3.13
	$7F_3$	331	68	20.58
	$7F_4$	0	2	0
		61	17	11.16

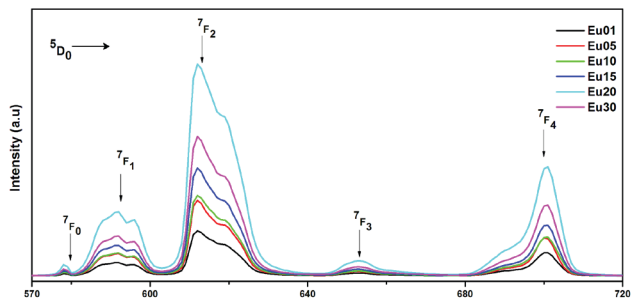


Figure 7: Emission spectra of europium doped zinc phosphate glass matrix for different concentrations